



Open Archive Toulouse Archive Ouverte (OATAO)

OATAO is an open access repository that collects the work of Toulouse researchers and makes it freely available over the web where possible.

This is an author-deposited version published in: <http://oatao.univ-toulouse.fr/>
Eprints ID : 3033

To link to this article :

URL : [http://dx.doi.org/10.1016/S0009-2509\(02\)00268-3_](http://dx.doi.org/10.1016/S0009-2509(02)00268-3_)

To cite this version : Mavros, Paul and Xuereb, Catherine and Fort, Ivan and Bertrand, Joël (2002) *[Investigation by laser doppler velocimetry of the effects of liquid flow rates and feed positions on the flow patterns induced in a stirred tank by an axial-flow impeller.](#)* Chemical Engineering Science, Volume 57 (n°18). pp.3939. ISSN 0009-2509

Any correspondence concerning this service should be sent to the repository administrator: staff-oatao@inp-toulouse.fr

Investigation by laser Doppler velocimetry of the effects of liquid flow rates and feed positions on the flow patterns induced in a stirred tank by an axial-flow impeller

Paul Mavros^{a,*}, Catherine Xuereb^b, Ivan Fořt^c, Joël Bertrand^b

^aDepartment of Chemistry, Aristotle University of Thessaloniki, Thessaloniki 54006, Greece

^bLaboratoire de Génie Chimique, UMR CNRS 5503-ENSIACET, Toulouse, France

^cDepartment of Chemical and Food Process Equipment & Design, Czech Technical University, Prague, Czech Republic

Abstract

The flow patterns established in a continuously-fed stirred tank, equipped with a Mixel TT axial-flow impeller, have been investigated by laser Doppler velocimetry, for a high and a low value of mean residence time—mixing time ratio. The pseudo-two-dimensional axial-radial-velocity vector plots, as well as the spatial distributions of the tangential velocity component and the velocity profiles around the impeller, show that the interaction between the incoming liquid and the liquid entrained by the agitator rotation cause the flow pattern in the vessel to become strongly three-dimensional, especially in the region between the plane, where the feeding tube lies, and the 180°-downstream plane. The increase in the liquid flow rate and the location of the feed entry both affect the flow pattern, with the latter having a more pronounced effect. The overall process, in this mode of operation, depends upon the appropriate configuration and choice of parameters: for conditions corresponding to high liquid flow rates, the flow patterns indicate the possibility of short-circuiting, when the liquid is fed into the stream being drawn by the agitator and when the outlet is located at the bottom of the vessel.

Keywords: Hydrodynamics; Mixing; Visualisation; Laser Doppler velocimetry; CSTR

1. Introduction

The design of stirred vessels, used for continuous-flow processes, has to take into consideration—compared to the batch stirred tanks—not only the type of agitator and other geometrical features of the vessel configuration, but two more factors related to the vessel hydrodynamics: the input and output locations of the incoming and outgoing streams:

- the outlet of the liquid may be
- (a) a single orifice, often positioned at the bottom of the vessel, to allow the draining of the contents by gravity and to ease the cleaning of the vessel,
- (b) through side openings, as often is the case in banks of adjacent square mechanically-agitated flotation cells, often used in flotation-cell banks, or

(c) by overflowing;

- the inlet point may also vary, with the tip of the feeding pipe located at the top of the vessel or at some place inside the stirred liquid, often close to the stirrer.

It is obvious that the positioning of these two points, in relation to the flow patterns induced by the agitator(s), will affect considerably the outcome of the process.

The time spent by the fluid inside the vessel may also affect the outcome of the process taking place inside the vessel, and this becomes important especially in cases of relatively fast reaction schemes. The mean residence or retention time (τ) is usually variable and depends upon the process taking place inside the vessel. However, it is customary to relate this to the mixing time (t_{mix}), i.e., the time necessary for the homogenisation of the vessel contents (in batch operation). A ratio of τ/t_{mix} of ~ 10 is usually considered appropriate for an effective operation of the continuous-flow

vessel (Mavros, Naude, Xuereb, & Bertrand, 1997; Zannoud, Guiraud, Costes, & Bertrand, 1991) although lower values have also been reported (Benayad, David, & Cognet, 1985).

For slow processes, it is obvious that the flowing-through liquid may be fed to the stirred vessel at any flow rate considered sufficient; however, in the case of relatively fast reaction schemes, the characteristic reaction time might compete with the characteristic flow time, i.e., the mean residence time, and in such cases a question may be raised, whether the continuous-flow stirred vessel may be operated in a “faster” mode, i.e., with an increased liquid flow rate and what would be, in that case, the limits of the operability of the vessel. At the same time, one could ask whether this operability would be also related to the geometrical configuration and the resulting hydrodynamics of the vessel, i.e., it would also depend on the type of agitator used, the flow pattern induced by it, and the location of the entry and exit points of the flowing-through liquid.

Although quite a few publications have dealt with several aspects of the operation of continuous-flow single- or multi-phase stirred vessels (see for example Greenhalgh, Johnson, & Howard, 1959; Patterson, 1975; Aubry & Villiermaux, 1975; Barthole et al., 1982; Benayad, David, & Cognet, 1985; Mahouast, David, & Cognet, 1987; Gaskey, Vacus, David, André, & Villiermaux, 1988; Gaskey, Vacus, David, & Villiermaux, 1990; Mahouast, 1991; Mahouast, Nardin, El Rhassouli, & Rondot, 1991; David & André, 1993; Houcine, Vivier, Plasari, David, & Villiermaux, 1994, 1996; Magelli, Nocentini, Orlandini, Fajner, & Pinelli, 1997; Konishi, Kogasaki, & Asai, 1997; Bomben, Selva, Tundo, & Valli, 1999; Distelhoff & Marquis, 1999, 2000) or similar process vessels, e.g., rotating-disk contactors (Fei, Wang, & Wan, 2000), as well as with the identification of the flow patterns in batch stirred vessels for various agitators using sophisticated experimental techniques like laser Doppler velocimetry (LDV), laser-induced fluorescence (LIF) and particle image velocimetry (PIV), among others (Mezaki, Mochizuki, & Ogawa, 2000; see also Mavros, Xuereb, & Bertrand (1996) and Mavros (2001) for an extensive list of related references), little work seems to have been done to investigate the low patterns in such vessels (see Kemoun et al., 1997; Mavros, Naude, Xuereb, & Bertrand, 1997; Zannoud, Guiraud Costes, & Bertrand, 1991; Mavros, Barrué, Xuereb, Fořt, & Bertrand, 2000).

In the previous work (Mavros, Naude, Xuereb, & Bertrand, 1997), the flow patterns in continuous-flow stirred vessels were investigated for only one liquid feed rate, with the liquid fed in the region corresponding roughly to the circulation “eye” in the upper part of the vessel; the emphasis was put rather on the comparison of the flow patterns for the batch and continuous-flow cases, as well as for the determination of the effect of the type of agitator used (radial or axial). In this work, the effect of the location of the feed position on the vessel hydrodynamics is studied again by

identifying the flow patterns using laser Doppler velocimetry; however, this is done for two different feed positions, in relation to two different flow rates. These results yield a qualitative assessment of the operability limitations of the continuous-flow stirred vessels.¹

2. Experimental apparatus and procedure

All velocity measurements were taken in a cylindrical vessel made of Perspex, with an i.d. (T) equal to 0.190 m; it was located inside a square transparent “box” filled with tap water, with a high-optical-quality glass (“altuglass”) window, which allowed the laser beams to focus inside the stirred liquid with minimal distortion. The vessel had a dished bottom, with a radius of curvature (R) equal to 0.190 m; it was equipped with four flat baffles having a width equal to $T/10$, mounted flush to the vessel wall and reaching the vessel bottom. The height of the liquid in the vessel (H) was kept constant at 0.190 m, resulting in a liquid volume (V_L) of $5.15 \times 10^{-3} \text{ m}^3$.

An axial-flow Mixel TT impeller ($D/T = \frac{1}{2}$) was used for all experiments (Fig. 1); its clearance—measured from its mid-plane to the bottom of the vessel—was kept constant at $C = T/2$. The motor used for the rotation of the agitator was equipped with a tachometer, allowing for the indication of the rotation speed (N). The shaft used for these measurements had an o.d. (d_S) equal to 0.008 mm and extended till the bottom of the vessel.

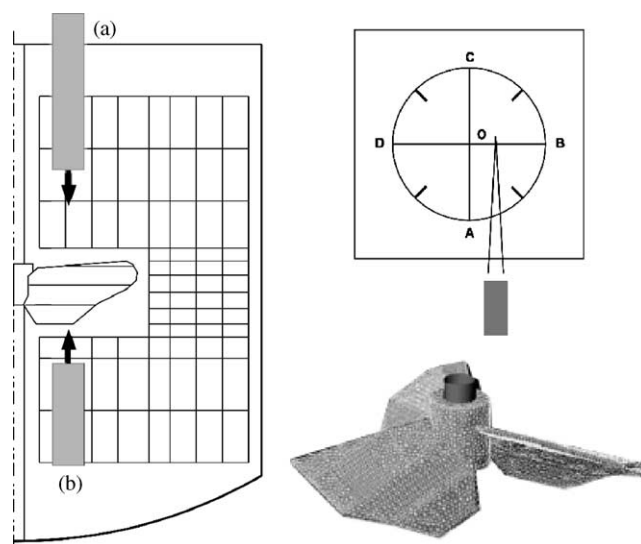


Fig. 1. (Left) location of liquid-feeding tubes. (a) Top feed. (b) Bottom feed. The grid indicates the locations of the LDV measurements in the upper and lower part of the vessel and at the side of the impeller. (Right) top: location of the planes for the LDV measurements in batch conditions; bottom: the Mixel TT impeller.

¹ Part of the work presented in this publication was presented at the 14th International Congress of Chemical and Process Engineering, CHISA, Prague, 27–31 August, 2000.

The liquid-feeding tube, made of copper, had an i.d. of 10 mm and an o.d. of 12 mm. Two sets of experimental results were obtained: in the first set, the tube tip was located above the impeller, at a distance of 48 mm from the liquid free surface and with the outer tube wall 11 mm from the agitator shaft (Fig. 1a, “a”); thus, the liquid entering the vessel joined co-currently the liquid being drawn in the impeller-swept region. In the second series, the tube was bent so that the tip was facing the stream flowing out of the impeller (Fig. 1a, “b”); in this case, the entering liquid flowed counter-currently to the flow discharged by the impeller. The liquid outlet for both series was located at the centre of the dished bottom of the vessel. In all cases, tap water was fed into the stirred vessel.

The laser Doppler apparatus consisted of:

- the laser source (Argon Spectra Physics mod. Stabilité 2017, power 4 W);
- the optical transmitter (Dantec mod. 60 * 41), which incorporated the beam splitter into one blue and one green beam,
- the Bragg cells and the connection with the optic fibres;
- the focusing unit (Dantec), with a lens of 600 mm, for the convergence and focusing of the laser beams inside the stirred tank;
- two photomultipliers (Dantec 57 * 28) operating in backscatter mode;
- a Flow Velocity Analyser (Dantec 58N20), which analysed the Doppler signal; and
- an oscilloscope, for the optical control of the signal quality.

Its dual beam allowed the simultaneous determination of two of the three velocity vector components (axial, radial, tangential).

From the instantaneous velocity (u_i , $i=r,z,t$) time series, the values of the mean (U_i) and the r.m.s. (u'_i) velocity were determined:

$$U_i = \frac{\sum_{k=1}^n t_k u_{ik}}{\sum_{k=1}^n t_k}, \quad u_{i,r.m.s.} = (\overline{u_i'^2})^{1/2} \\ = \left(\frac{\sum_{k=1}^n t_k (U_i - u_i)^2}{\sum_{k=1}^n t_k} \right)^{1/2}, \quad i = r, z, t. \quad (1)$$

This calculation takes into account the seeding-particle higher-velocity bias, by including in the calculations the time (t_k) that the seeding particle spends in the measuring volume (for a description of the bias effect and the necessity for correction see also Fingerson & Menon (1998); Adrian (1996); Edwards & Meyers (1984), and Buchave, George, & Lumley (1979), among others).

From the r.m.s. velocities, it is possible to calculate the local turbulent kinetic energy (k) and the turbulence intensity (Tu), which is a measure of the importance of the

velocity fluctuations:

$$k = \frac{u_{r,r.m.s.}^2 + u_{z,r.m.s.}^2 + u_{t,r.m.s.}^2}{2}, \\ Tu = \left(\frac{u_{r,r.m.s.}^2 + u_{z,r.m.s.}^2 + u_{t,r.m.s.}^2}{U_r^2 + U_z^2 + U_t^2} \right)^{1/2}. \quad (2)$$

When studying batch-condition flow patterns by LDV in fully baffled cylindrical vessels, it is usually assumed that the flow is stationary, i.e., it is possible to combine the radial velocity (U_r) taken at the side plane (Fig. 1b: line “OB”) with the tangential velocity (U_t) obtained at the “front” plane (Fig. 1b: line “OA”) (the axial velocity component U_z may be taken from either set of measurements, since these should in principle coincide) to yield the local velocity vector for those planes. In the present experimental set-up, the presence of the feeding tube removes the axial symmetry. However, it is still possible to maintain a kind of “stationarity” by adjusting the location of the feeding tube plane in relation to the velocity-measuring plane: it is postulated that similar hydrodynamic conditions prevail, when tangential and axial velocities are measured in the “front” plane (Fig. 1b: line “OA” and Fig. 2b) while the feeding tube is in the side plane (line “OB”), and when radial and axial velocities are measured in the side plane (Fig. 1b, line “OB”) while the feeding tube is the back plane (Fig. 1b: line “OC” and Fig. 2c). Thus, if the tangential velocity component is measured in the “front” plane while the feeding tube is in the side plane (Fig. 2b) and the radial component is measured in the side plane with the feeding tube moved to the plane “behind” the agitator shaft (Fig. 2c)—with the axial velocity component taken from either plane—a full set of three-component velocity vectors is obtained for the plane which lies 90° downstream from the plane, where the feeding tube is located. In a similar way, it is possible to obtain a set of velocity measurements for 180°-downstream conditions, with the feeding tube always positioned in a plane 180° upstream from the measuring plane.

For the determination of the operating conditions, it was necessary to estimate the mixing time; the mean residence time is easily obtained from the ratio:

$$\tau = \frac{V_L}{F_L}. \quad (3)$$

The dimensionless mixing time (Nt_{mix}) has been correlated with various process parameters, but mainly with the vessel and impeller diameters, the power consumption (Nienow, 1997; Ruszkowski, 1994) or the width and number of blades (Sano & Usui, 1987); the following simple relation is claimed to estimate it with satisfactory accuracy (Roustan & Pharamond, 1988; Tatterson, 1991), regardless of the type of agitator:

$$Nt_{mix} = 4 \left(\frac{T}{D} \right)^2. \quad (4)$$

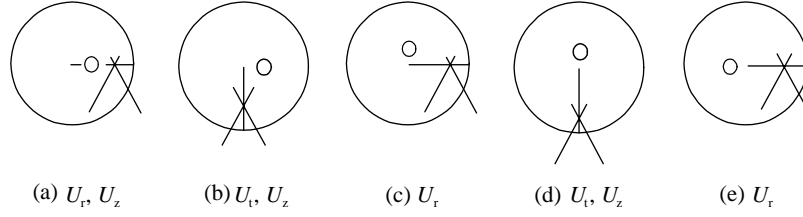


Fig. 2. Combination of velocity measurements in various planes, in relation to the feeding tube position, to obtain either the two-component (u_{rz}) or the three-component (u_{rzt}) velocity vector: (a) measurement of the radial and axial velocity components in the feed plane; (b) measurement of the axial and tangential velocity components in the 90° -in-front (downwards) plane; (c) measurement of the radial velocity component in the 90° -in-front (downwards) plane; (d) measurement of axial and tangential velocity components in the 180° -in-front (downwards) plane; (e) measurement of the radial velocity component in the 180° -in-front (downwards) plane.

Table 1

Experimental conditions ($F_L = 2.017 \times 10^{-4} \text{ m}^3 \text{ s}^{-1}$)

Feed direction		$N = 6 \text{ Hz}, \tau/t_m = 9.6, Re = 27100$				$N = 3 \text{ Hz}, \tau/t_m = 4.8, Re = 54200$			
		Co-current		Counter-current		Co-current		Counter-current	
		min	max	min	max	min	max	min	max
V_r^*	batch	0.050	0.109	NA ^a		NA		NA	
	feed plane	-0.055	0.107	-0.072	0.103	-0.088	0.101	-0.165	0.145
	90° -downstream	-0.063	0.080	-0.014	0.160	-0.082	0.086	-0.069	0.165
	180° -downstream	-0.073	0.089	-0.038	0.082	-0.079	0.080	-0.047	0.048
V_z^*	batch	0.090	0.205	NA		NA		NA	
	feed plane	-0.149	0.629	-0.474	0.142	-0.212	1.507	-0.734	0.115
	90° -downstream	-0.124	0.200	-0.046	0.173	-0.166	0.209	-0.052	0.216
	180° -downstream	-0.101	0.215	-0.100	0.219	-0.091	0.198	-0.056	0.182
V_t^*	batch	0.048	0.100	NA		NA		NA	
	feed plane	NM ^b		NM		NM		NM	
	90° -downstream	-0.035	0.137	-0.039	0.089	-0.091	0.095	-0.166	0.138
	180° -downstream	-0.031	0.105	-0.037	0.121	-0.071	0.111	-0.051	0.119
Tu	batch	0.5	4.6	NA		NA		NA	
	feed plane	NC ^c		NC		NC		NC	
	90° -downstream	0.5	6.1	0.6	6.3	0.5	3.0	0.5	4.7
	180° -downstream	0.5	4.8	0.5	14.8	0.6	6.9	0.6	17.0
k^*	batch	0.001	0.009	NA		NA		NA	
	feed plane	NC		NC		NC		NC	
	90° -downstream	0.001	0.024	0.001	0.016	0.001	0.014	0.002	0.036
	180° -downstream	0.001	0.009	0.0003	0.010	0.001	0.011	0.001	0.013

Radial velocities are positive outwards (towards the vessel walls), axial velocities are positive downwards, and tangential velocities are positive clock-wise. Negative velocities indicate flow in the opposite direction.

^aNM: not measured.

^bNC: not calculated.

^cNA: not applicable.

Hence, the ratio of the two characteristic times (τ/t_{mix}) becomes

$$\frac{\tau}{t_{\text{mix}}} = \frac{V_L/F_L}{(4/N)(\frac{T}{D})^2} = \frac{V_L}{4} \left(\frac{T}{D}\right)^{-2} \left(\frac{N}{F_L}\right). \quad (5)$$

It is obvious from Eq. (5) that, by keeping the volumetric flow rate (F_L) constant and changing the impeller rotation frequency, it is possible to alter the characteristic time ratio (τ/t_{mix}). Table 1 gives the values of the impeller rotation

frequency chosen for the velocity measurements and the corresponding time ratios.

In these hydrodynamic conditions, two main liquid flow rates compete: the incoming liquid jet, and the jet being ejected by the rotating impeller. In terms of flow, since the Mixel TT has a flow number of $Fl = 0.67$ (Aubin, Mavros, Fletcher, Bertrand, & Xuereb, 2001; Mavros & Bertrand, 2002), the experimental conditions of Table 1 correspond to a discharged volumetric flow rate ranging from $Q_p = 1.72 \times 10^{-3} \text{ m}^3 \text{ s}^{-1}$ (for $N = 3 \text{ Hz}$) to $Q_p = 3.45 \times 10^{-3} \text{ m}^3 \text{ s}^{-1}$

(for $N = 6$ Hz). Therefore, the incoming liquid flow rate ($\cong 2.02 \times 10^{-4} \text{ m}^3 \text{ s}^{-1}$) corresponds to approximately 6–12% of the pumped-out liquid flow rate. In terms of velocity magnitudes, the mean velocity of the liquid at the exit of the feed tube, $U_{\text{tube}} (= F_L/A_{\text{tube}} = 2.017 \times 10^4/7.85 \times 10^{-5} \cong 2.6 \text{ m s}^{-1})$, is of the same order of magnitude as the agitator blade tip speed at the higher rotation frequency, $U_{\text{tip}} \cong 1.8 \text{ m s}^{-1}$ ($N = 6$ Hz), but about 3 times higher than U_{tip} at the lower rotation frequency: $U_{\text{tip}} = 0.90 \text{ m s}^{-1}$ ($N = 3$ Hz); thus, it is probable that at the higher volumetric flow rate the incoming jet will affect the flow patterns. In terms of energy input, the agitated liquid receives energy on the one hand from the rotating impeller with an average energy input per unit mass given by the following equation:

$$\varepsilon_{\text{agit}} = \frac{P}{m} = \left(\frac{Po D^5}{V_L} \right) N^3 \quad (6)$$

and, on the other hand, also from the incoming liquid:

$$\varepsilon_{\text{kin}} = \frac{1}{2} \frac{F_L U_{\text{tube}}^2}{V_L}. \quad (7)$$

Using the power number for the Mixel TT: $Po = 0.67$, which was determined in batch conditions (Aubin, Mavros, Fletcher, Bertrand, & Xuereb, 2001; Mavros & Bertrand, 2002), we may estimate the power input due to the impeller: for the lower rotation frequency ($N = 3$ Hz), $\varepsilon_{\text{agit}} = 0.027 \text{ W kg}^{-1}$, while for the higher one ($N = 6$ Hz), $\varepsilon_{\text{agit}} = 0.217 \text{ W kg}^{-1}$. Since the flow rate is kept constant, in both

cases $\varepsilon_{\text{kin}} = 0.132 \text{ W kg}^{-1}$. Therefore, in the case of the high times ratio ($\tau/t_{\text{mix}} = 9.6$; $N = 6$ Hz), the energy input due to the rotating impeller is twice as high as the power input by the incoming liquid. When the rotation frequency is lowered ($N = 3$ Hz; $\tau/t_{\text{mix}} = 4.8$), this situation is reversed and the energy input from the incoming jet is about 5 times higher than the power input by the rotating impeller.

In conclusion, the “intensification” of the vessel usage—as seen by the decrease in mean residence time—corresponds to a hydrodynamic situation where the incoming liquid jet has a higher tube-tip velocity than the agitator-tip velocity, and a considerable difference in power input.

3. Results and discussion

3.1. Flow patterns

In the following figures, the spatial distributions of velocities in the various planes inside the stirred vessel are presented graphically. The flow maps are colour-coded, with the highest (positive) velocity represented by red and the lowest velocity (negative) with blue colour. The direction convention for these figures is as follows: radial velocities are positive towards the vessel walls (\rightarrow), axial velocities are positive downwards (\downarrow) and tangential velocities are positive clockwise (\curvearrowright).

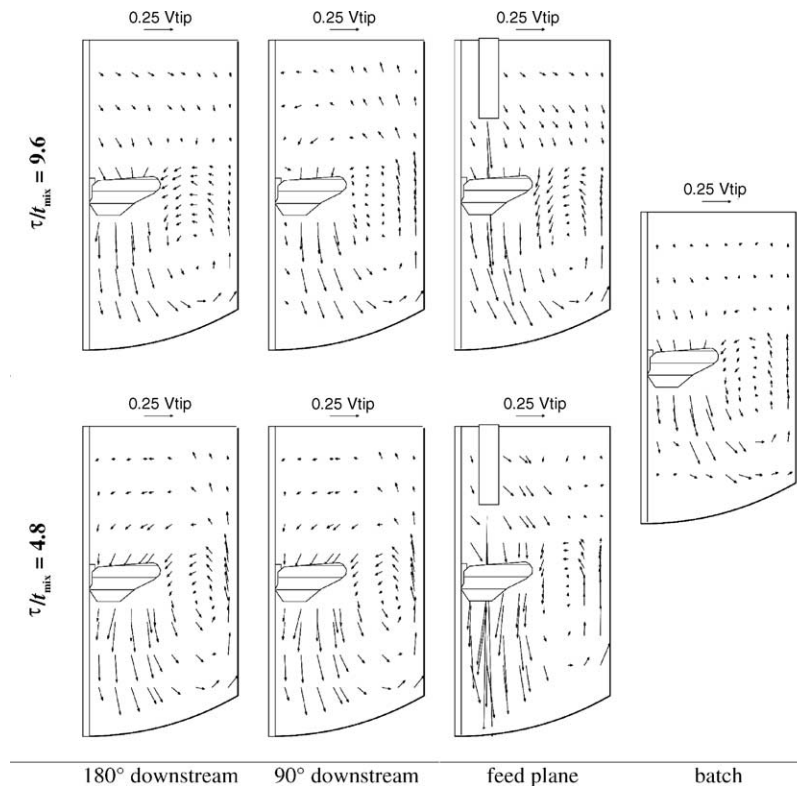


Fig. 3. Pseudo-2D flow patterns in the stirred vessel for a high and a low mean residence time; liquid feed in the upper part of the vessel (co-current feed).

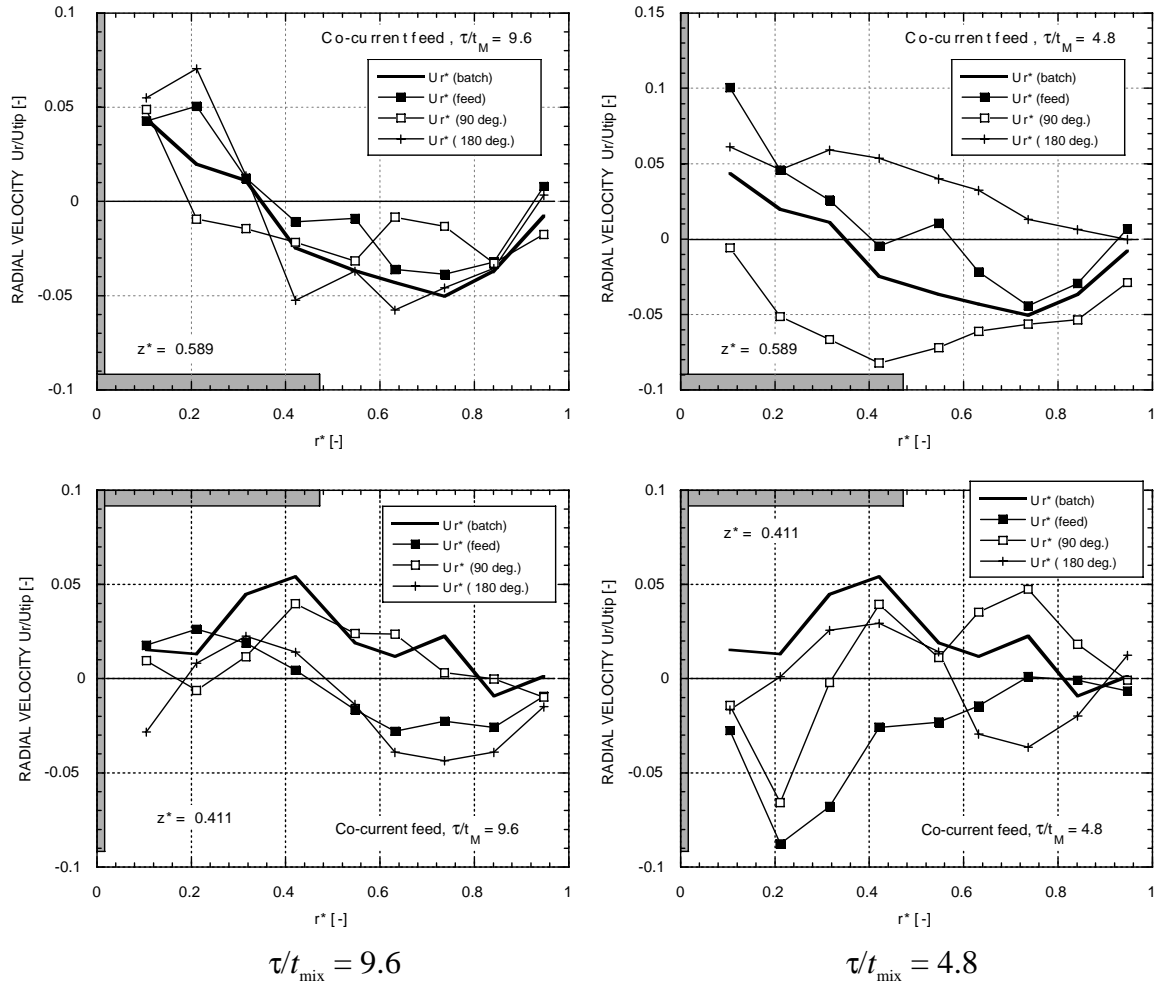


Fig. 4. Profiles of radial velocities on the upper and lower sides of the impeller for the co-current feed configuration.

3.1.1. Co-current feed

In the first experimental series, the liquid incoming flow was introduced above the impeller in the region where previous measurements in batch conditions (Mavros et al., 1996) had shown that the liquid is sucked in the impeller region by the pumping-in action of the rotating stirrer; therefore, the incoming flow was co-current with the local circulating liquid. Fig. 3 shows the pseudo-2-D flow maps in the feed plane, the 90° and the 180°-downstream planes. For the high times ratio ($\tau/t_{\text{mix}} = 9.6$), the entering liquid jet is seen passing through the impeller-swept volume, as the high axial velocities just below the TT indicate. However, the strong circulatory flow induced by the axial agitator does not seem to be considerably affected: the flow loop structure around the TT seems similar to the one observed in the batch case (also shown in Fig. 3). A region of slightly faster up-flowing liquid is noticed in the 90°-downstream plane close to the upper part of the vessel walls, and an increase in velocity magnitudes beneath the TT is also noticeable in all three planes.

It is interesting to note that radial velocities just above the agitator have similar magnitudes in all planes (Fig. 4), and that they are comparable to the batch case velocities. Beneath the impeller, the changes are more important: whereas in the batch case radial velocities are positive, i.e., the flow is directed towards the vessel walls, in the case of the continuous flow the flow appears directed towards the centre of the vessel both for the feed plane and the 180°-downstream one. The axial velocity distribution (Fig. 5) shows, as expected, a peak at the region where the incoming jet reaches the impeller-swept volume, but otherwise the profiles are similar to the batch case one both over and beneath the stirrer. The tangential velocity distributions (Fig. 6) show that the strong circulatory flow induced by the impeller rotation is maintained with only slight changes: whereas in the batch case a tangential movement is noticeable also at the upper edge of the impeller, in the two downstream planes the tangential flow is reduced to the lower part of the vessel, while in the upper part the magnitudes of U_t^* are very low and close to zero, with regions close to the impeller shaft and

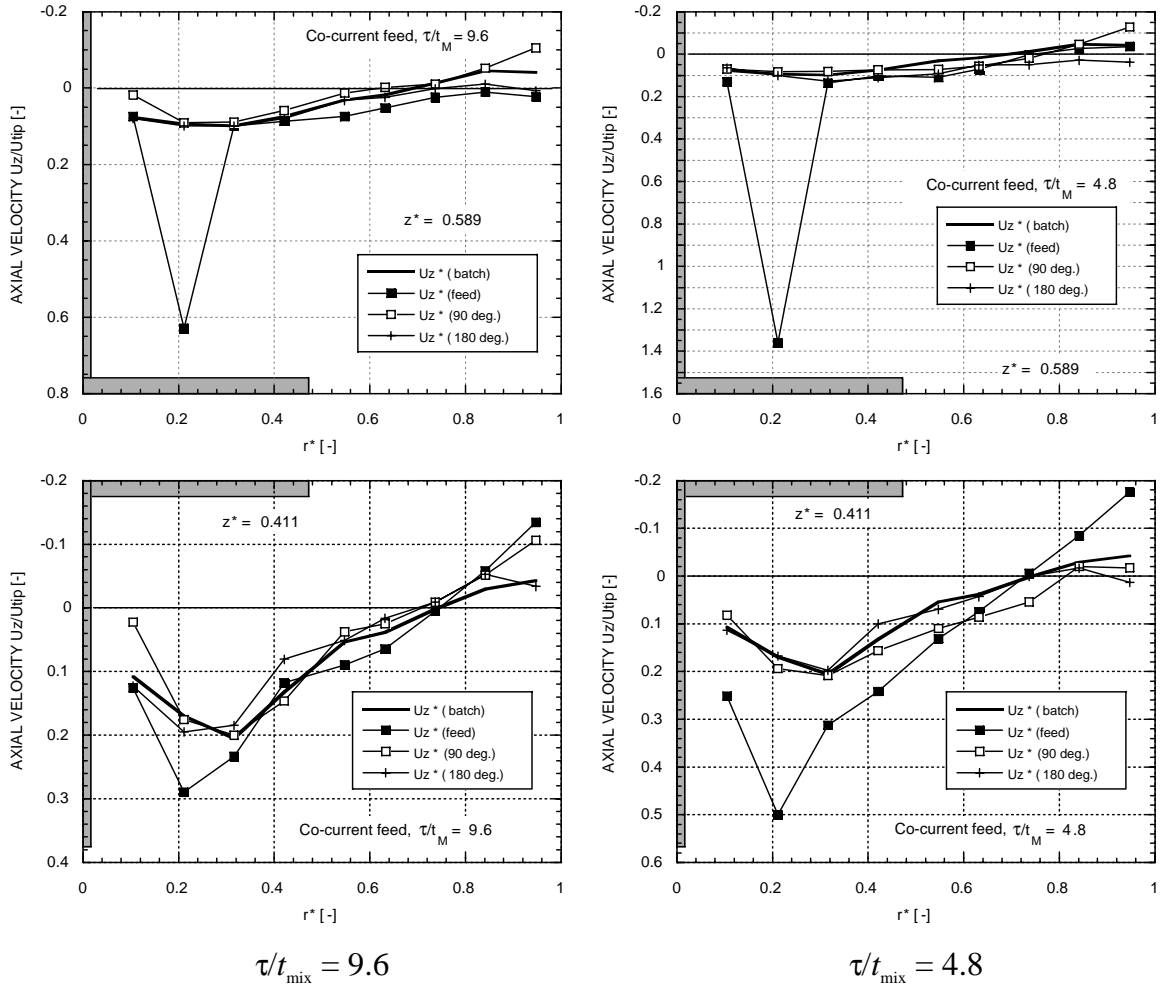


Fig. 5. Profiles of axial velocities on the upper and lower sides of the impeller for the co-current feed configuration.

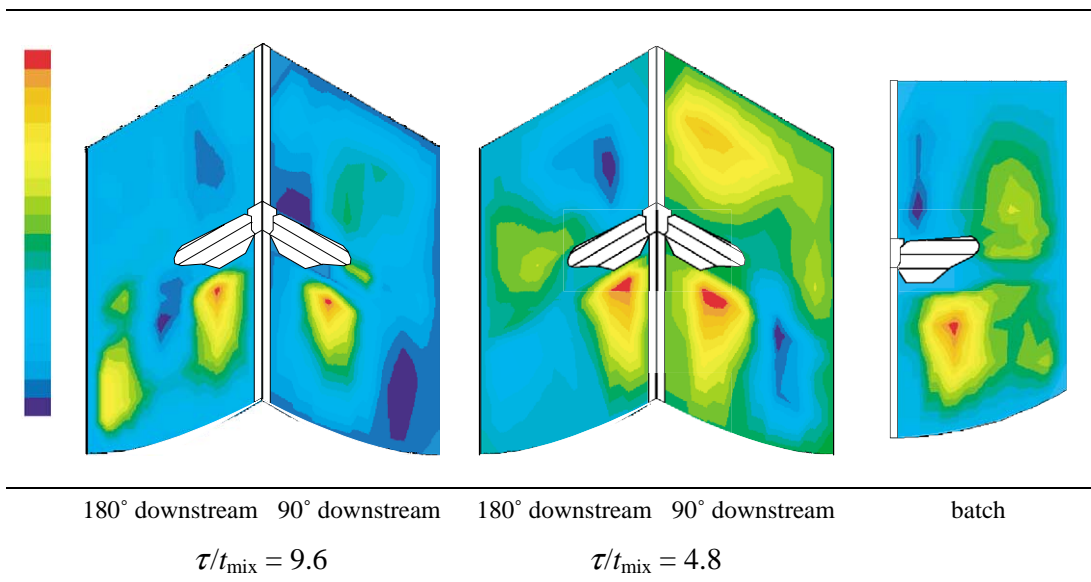


Fig. 6. Spatial distribution of dimensionless tangential velocities (U_t^*) in the 90°-downstream and 180°-downstream planes for liquid feed in the upper part of the vessel (co-current feed).

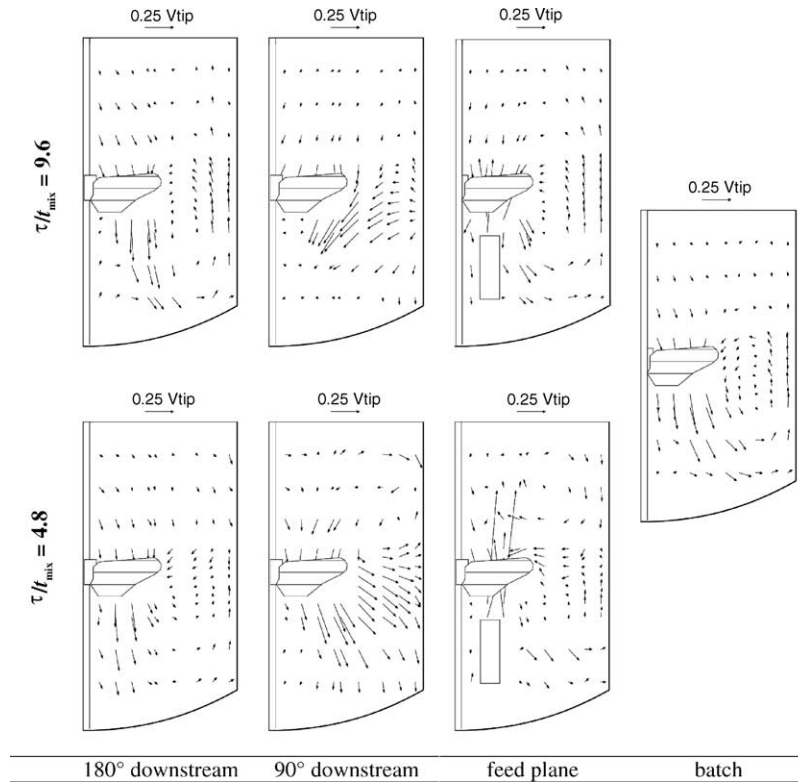


Fig. 7. Pseudo-2D flow patterns in the stirred vessel for a high and a low mean residence time; liquid feed in the lower part of the vessel (counter-current feed).

the lower edge of the TT (in the 180° -plane) even showing liquid rotating in a counter-clockwise direction, albeit with very small magnitudes (shown in Table 1). It seems, therefore, that for slow through flows, i.e., when the liquid mean residence time is high, compared to the mixing time, the single-loop flow structure usually induced by the axial-flow TT is maintained.

When the mean residence time is lowered, i.e., more liquid flows through the stirred vessel, the flow structure seems to be affected for the co-current feed in the feed plane, with very high velocities noticed in the lower part of the vessel, which are directed towards the exit opening of the vessel (Fig. 3, lower part). For the two subsequent planes, i.e., the one 90° and the other 180° downstream, the flow pattern seems to have recovered its usual loop structure around the impeller with high downward velocities noticeable beneath the agitator in these planes, too. These high velocities are probably a clear indication of liquid being “siphoned” directly out of the vessel, bypassing the bulk of the liquid vessel contents. The radial velocity profile above the impeller (Fig. 4) appears strongly affected mainly in the 180° -downstream plane: whereas in the other planes the radial flow is mostly negative, i.e., directed towards the centre of the vessel; in this plane it is all positive, indicating outwards-flowing liquid. The axial velocity profiles are interesting (Fig. 5) because the peak beneath the tube tip appears not only above the impeller but also beneath it,

indicating that the jet passes clearly through the impeller-swept region. The tangential flow maps (Fig. 6) also show some disruption: while a region of strong clockwise liquid rotation is still visible beneath the agitator, another region appears in both the 90° and the 180° downstream planes with liquid flowing counter-clockwise—indicated by the deep blue colour and with velocity magnitudes (shown in Table 1) of 3.5% of U_{tip} and 9.1% of U_{tip} , for the two planes, respectively.

Combining these results, it may be concluded that for the co-current feed configuration, the increase in liquid flow-through rate results in a probable decrease in vessel operability, with a clear indication of liquid bypassing the bulk of the liquid and flowing directly to the exit of the vessel. It is therefore recommended that for such a configuration, the mean residence time of the flowing-through liquid should be maintained high.

3.1.2. Counter-current feed

In the second experimental series, the incoming flow was introduced below the impeller so that the incoming flow would be directed against the flow being pumped out by the impeller.

For both high and low mean residence time cases, the disruption of the flow pattern is clearly considerable (Fig. 7). For $\tau/t_{mix} = 9.6$, the feed-plane 2-D map seems similar to the batch case; in fact, the incoming flow is diverted

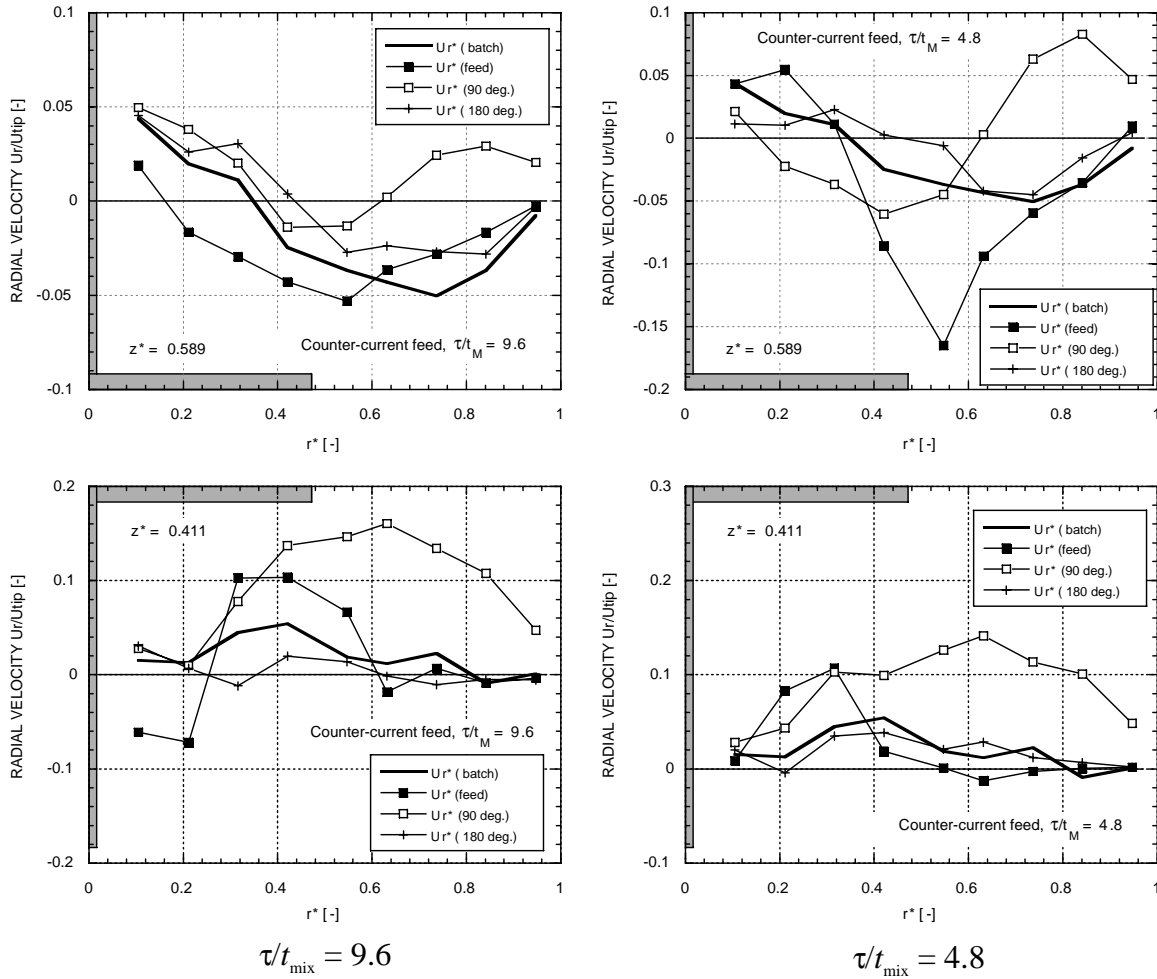


Fig. 8. Profiles of radial velocities on the upper and lower sides of the impeller for the counter-current feed configuration.

by and into the strong tangential flow beneath the TT. In the 90° -downstream plane, the usual toroidal flow structure around the TT is lost: the flow is observed flowing radially inwards and downwards, with the flow in the upper part of the vessel unperturbed. In the 180° -downstream plane, the usual TT flow structure is re-established, with the flow loop exiting from beneath the agitator-swept volume and entering it from above, and a small secondary flow loop at the bottom of the vessel.

The effect on radial velocities is more important beneath the agitator (Fig. 8), where higher velocities are observed at the 90° plane, indicating a strong outward radial movement of the liquid. Axial velocities, on the other hand, are not considerably affected (Fig. 9), similar to the co-current feed case (Fig. 5). A similar result is observed with the tangential velocity map (Fig. 10): the region with high velocities appears moved slightly outwards, but otherwise it remains close to the lower impeller edge. Interestingly, the counter-rotating tangential velocities have magnitudes comparable to the co-rotating ones (Table 1), especially in the 180° -downstream plane, indicating that the region in the upper part of the vessel and between the 90° and the

180° downstream planes may have a highly complex flow structure resembling a liquid “sink”.

The decrease of the characteristic times ratio ($\tau/t_{\text{mix}}=4.8$) again has spectacular results. The liquid jet crosses again the impeller-swept region, seen both in the 2-D flow map (Fig. 7) and the profiles of axial velocities (Fig. 9); a large secondary flow loop is thus established in the upper part of the vessel, clearly seen in the feed plane. Visual observation of the stirred vessel indicated also that the incoming liquid jet reached the surface of the liquid, with a periodic “eruption” corresponding to the passage of the agitator blades.

The entering liquid is obviously entrained outwards by the rotating tangential flow (seen by the increase of the region of high clockwise-rotating tangential velocities in Fig. 10), hence the radial velocity profile changes observed, especially in the feed and the 90° -downstream planes (Fig. 8), which result in the TT appearing as a radial agitator in this plane (see the 2-D flow map in Fig. 7). The axial flow structure is partially re-established at the 180° -downstream plane, although the composite axial-radial velocity magnitudes appear small in comparison to the other planes and the batch case. It is interesting to note that the tangential flow appears stronger

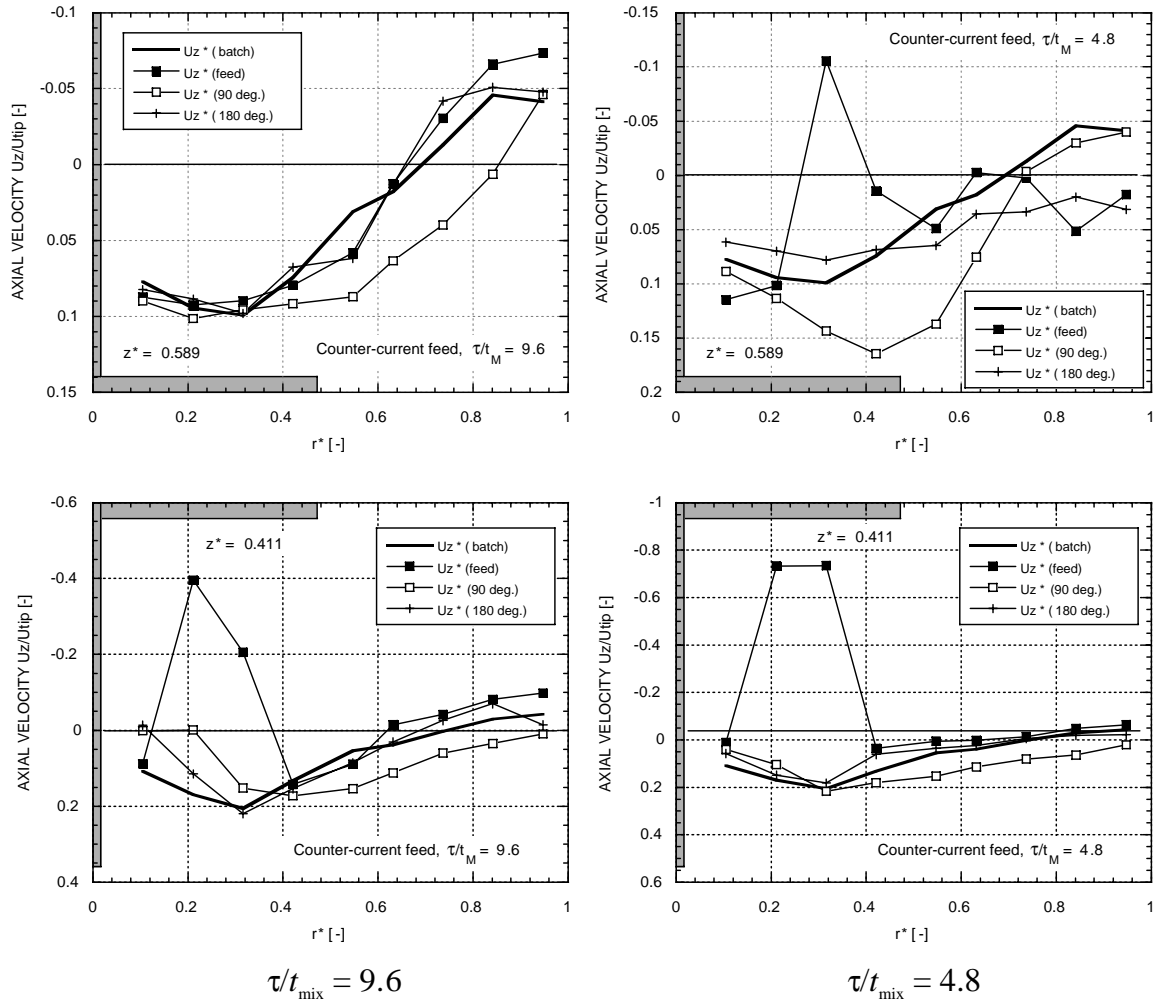


Fig. 9. Profiles of axial velocities on the upper and lower sides of the impeller for the counter-current feed configuration.

in the counter-clockwise direction in the 90° -downstream plane, as indicated by the U_i^* values in Table 1.

It may be concluded, therefore, that the counter-current feed of the liquid seems to avoid the short-circuiting caused by the location of the vessel outlet at the bottom of the vessel.

3.2. Turbulence characteristics

Fig. 11 presents the turbulence intensity (Tu) which was calculated from the velocities measured in the two downstream planes (90° and 180°). Regions of high Tu values usually indicate slow velocities, where the liquid exhibits a tendency to often switch direction.

In the case of the co-current feed (into the impeller-drawn stream), the highest turbulence intensity appears next to the agitator edge in the 90° plane, but moves further up and close to the vessel walls in the 180° plane; the latter resembles more the situation observed in the batch case (also shown in the same figure), although less distributed than that. When the characteristic times ratio increases, the

turbulence intensity appears practically the same in both the downstream planes.

In the case of the counter-current feed, the turbulence intensity distribution differs considerably from the batch case or from the co-current feed (Fig. 11). The regions of high direction uncertainty and high switching probability appear, for the high τ/t_{mix} ratio, below the impeller, at the 90° plane, and far away, at the top of the vessel walls at the 180° plane. When the times ratio is decreased, the flow pattern changes and the high-turbulence area appears in the 180° plane at the edge of the impeller, showing again the regions of slow and somehow fast-direction-change flow.

Fig. 12 present the turbulent kinetic energy (k^* —rendered dimensionless by dividing k with U_{tip}^2) distribution in the two downstream planes; k^* is usually used to estimate the local energy dissipation rate. In the batch case, the highest values of k^* are found in the stream ejected by the axial-flow agitator, as is the case for other agitators too (Mavros et al., 1996). For the co-current feed configuration, the same pattern is maintained for both times ratios, indicating that

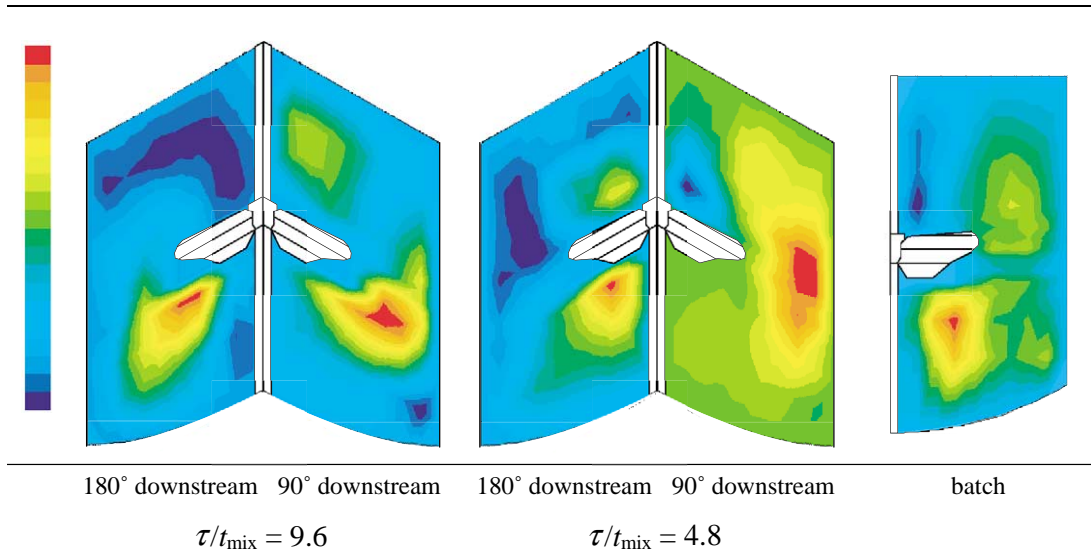


Fig. 10. Spatial distribution of dimensionless tangential velocities (U_t^*) in the 90° -downstream and 180° -downstream planes for liquid feed in the lower part of the vessel (counter-current feed).

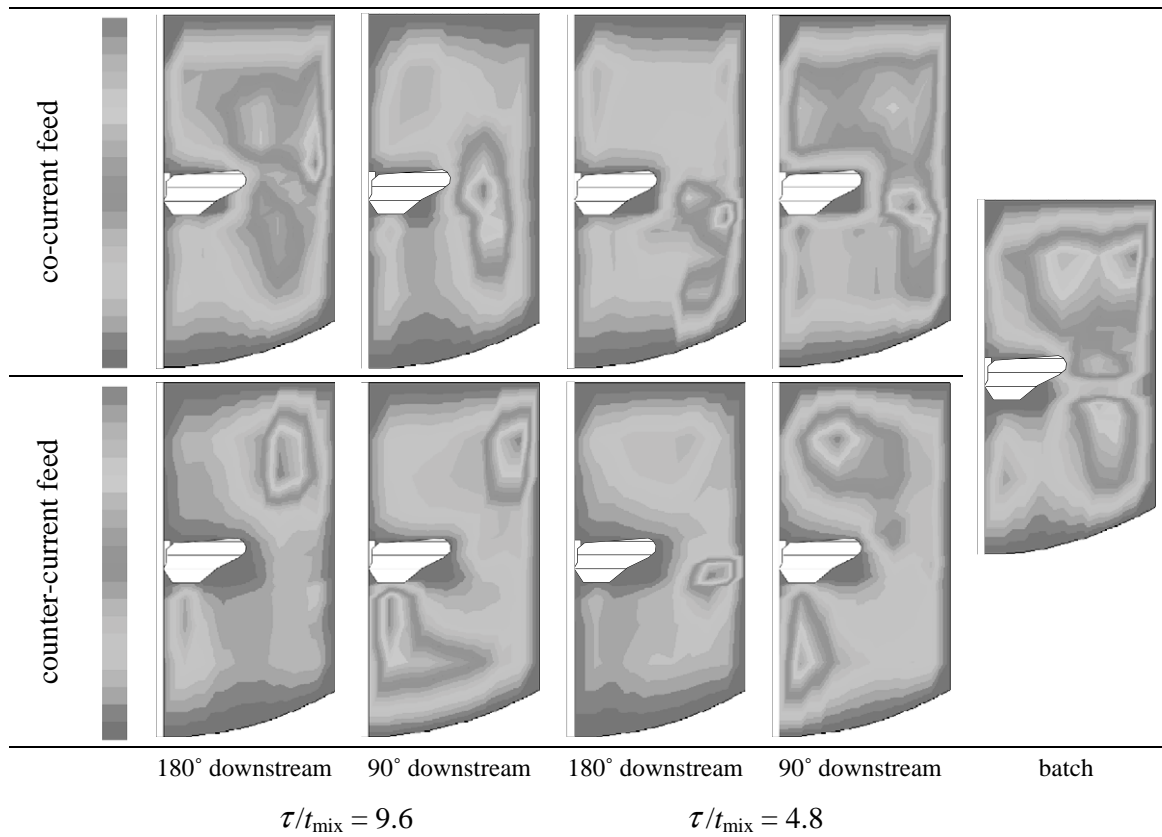


Fig. 11. Spatial distribution of the turbulence intensity (Tu) in the 90° -downstream and 180° -downstream planes for liquid feed in the upper (co-current feed) and the lower part of the vessel (counter-current feed).

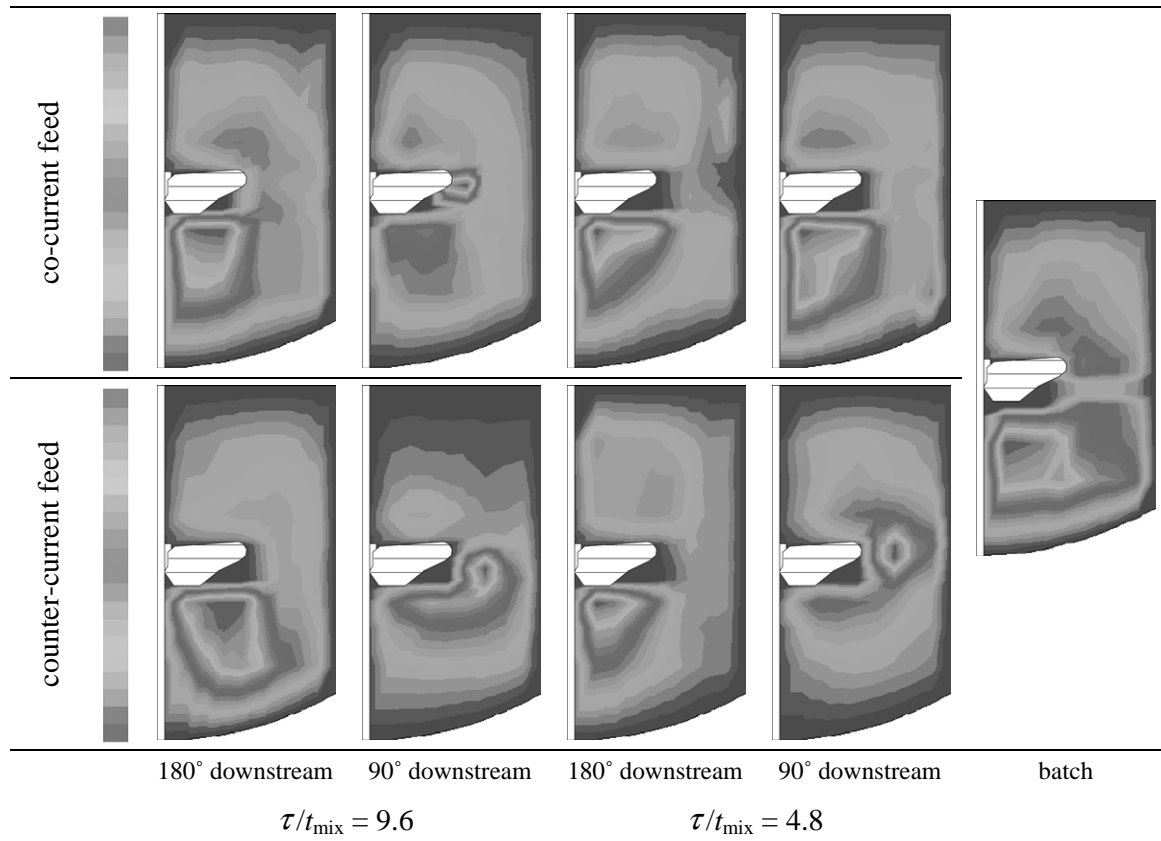


Fig. 12. Spatial distribution of the dimensionless turbulent kinetic energy ($k^* = k/U_{\text{tip}}^2$) in the 90° -downstream and 180° -downstream planes for liquid feed in the upper (co-current feed) and the lower part of the vessel (counter-current feed).

the most intensive flow remains in the region underneath the impeller. In the case of the counter-current feed, it is interesting to note that the spatial distributions lead to similar conclusions regarding the complex flow patterns: for both the high and the low characteristic times ratios, the region of highest energy dissipation in the 90° -downstream plane occurs *next* to the agitator and not *underneath* it. However, as the flow proceeds tangentially, it recovers its usual flow pattern and in the 180° -downstream plane the highest values of k^* appear again beneath the TT.

4. Conclusions

Laser Doppler velocimetry has been used to measure velocities in a continuous-flow stirred tank, agitated by an axial-flow agitator (Mixel TT). The measurements were taken for two values of the mean residence time—mixing time ratio, corresponding to a “typical” and an enhanced utilisation of the stirred vessel, and for two different locations of the liquid entry, the one feeding the liquid into the stream being pumped in by the impeller (“co-current” configuration), and the other feeding it against the stream being ejected by the impeller (“counter-current” configuration). The exit opening was located in all cases at the bottom of the vessel.

The results indicate that, in the case of the co-current feed, the decrease of the mean residence time of the flowing-through liquid may lead to problems of short-circuiting and bypassing, due to the location of the entry and exit pipes. In contrast, the counter-current feed did not show such potential problems. However, further work is necessary to investigate—experimental and possibly also numerically, using an appropriate CFD code—the limits of operability of the continuous-flow stirred tank.

The analysis of the flow patterns indicate also that the effects of the incoming liquid stream are noticeable mainly in the region close to the feeding pipe, and the flow patterns usually found in the batch case are found in the plane located 180° downstream from the feeding-tube plane.

Notation

A_{tube}	feed tube cross-sectional area, m^2
C	impeller clearance from the vessel bottom (measured from the impeller mid-plane), m
D	impeller diameter, m
d_S	agitator shaft diameter, m
Fl	flow number, dimensionless
F_L	liquid flow rate, $\text{m}^3 \text{s}^{-1}$

H	liquid height in vessel, m
k	turbulent kinetic energy, $\text{m}^2 \text{s}^{-2}$
m	mass of liquid in the vessel, kg
N	impeller rotation frequency, Hz
P	power, W
Po	power number, dimensionless
Q_p	liquid flowrate pumped out by the impeller, $\text{m}^3 \text{s}^{-1}$
r	radius, m
R	radius of curvature of vessel bottom, m
t_k	time spent by the seeding particle in the LDV-measuring volume, s
T	vessel diameter, m
Tu	turbulence intensity, dimensionless
t_{mix}	mixing time, s
u	r.m.s. velocity, $\text{m}^2 \text{s}^{-1}$
u'	instantaneous velocity, $\text{m}^2 \text{s}^{-1}$
U	mean velocity, $\text{m}^2 \text{s}^{-1}$
U_{tip}	impeller-blade tip velocity, $\text{m}^2 \text{s}^{-1}$
U_{tube}	liquid velocity at the tip of the feeding tube, $\text{m}^2 \text{s}^{-1}$
V_L	liquid volume, m^3
z	height, m

Greek letters

ε	energy dissipation, W
ρ	liquid density, kg m^{-3}
τ	mean residence time, s

Indices

agit	agitator
kin	kinetic
r	radial
t	tangential
z	axial

Acknowledgements

Thanks are due to Dr. H. Barrué for her help in the preparation of the graphic files. One of the authors (PM) acknowledges the financial support of this work by the EU (contract BRITE EURAM III BRRT-CT97-5035), while IF acknowledges the financial support of this work by the Czech Republic Ministry of Education (Research Project J04/98:212200008).

References

- Adrian, R. J. (1996). Laser velocimetry, In R. J. Goldstein (Ed.), *Fluid mechanics measurements* (pp. 175–299). Washington, DC: Taylor & Francis.
- Aubin, J., Mavros, P., Fletcher, D. F., Bertrand, J., & Xuereb, C. (2001). Effect of axial agitator configuration (up-pumping, down-pumping, reverse rotation) on flow patterns generated in stirred vessels. *Chemical Engineering Research and Design A*, 79(8), 845–856.
- Aubry, C., & Villermaux, J. (1975). Representation du melange imparfait de deux courants de reactifs dans un réacteur agité continu. *Chemical Engineering Science*, 30, 457–464.
- Barthole, J. -P., Maisonneuve, J., Gence, J. N., David, R., Mathieu, J., & Villermaux, J. (1982). Measurement of mass transfer rates, velocity and concentration fluctuations in an industrial stirred tank. *Chemical Engineering Fundamentals*, 1, 17–26.
- Benayad, S., David, R., & Cognet, G. (1985). Measurement of coupled velocity and concentration fluctuations in the discharge flow of a Rushton turbine in a stirred tank. *Chemical Engineering Processing*, 19, 157–165.
- Bomben, A., Selva, M., Tundo, P., & Valli, L. (1999). A continuous-flow o-methylation of phenols with dimethyl carbonate in a continuously fed stirred tank reactor. *Industrial Engineering and Chemistry Research*, 38(3), 2075–2079.
- Buchave, P., George, W. K., & Lumley, J. L. (1979). The measurement of turbulence with the laser Doppler anemometer. *Annual Review of Fluid Mechanics*, 11, 443–503.
- David, R., & André, C. (1993). Comparison of single and double inert tracer fluctuation measurements in a continuous stirred tank. *Chemical Engineering Technology*, 16, 234–237.
- Distelhoff, M. F. W., & Marquis, A. J. (1999). Scalar mixing measurements in a continuously operated stirred tank agitated with a Rushton turbine using a LIF line scan technique. In H. Benkreira (Ed.), *Fluid mixing* (IChemE Symposium Series Number 146). Vol. 6 (pp. 147–158). Rugby: IChemE.
- Distelhoff, M. F. W., & Marquis, A. J. (2000). Scalar mixing in the vicinity of two disk turbines and two pitched blade impellers. *Chemical Engineering Science*, 55(10), 1905–1920.
- Edwards, R. V., & Meyers, J. F. (1984). An overview of particle sampling bias. *Proceedings of the Second international symposium applications of laser anemometry to fluid mechanics* (11pp). Lisbon, Portugal, July 2–4.
- Fei, W. Y., Wang, Y. D., & Wan, Y. K. (2000). Physical modelling and numerical simulation of velocity fields in rotating disc contactor via CFD simulation and LDV measurement. *Chemical Engineering Journal*, 78, 131–139.
- Fingerson, L. M., & Menon, R. K. (1998). Laser Doppler velocimetry. In R. W. Johnson (Ed.), *The handbook of fluid mechanics* (pp. 35.1–35.18). Boca Raton, FL: CRC Press, Springer.
- Gaskey, S., Vacus, P., David, R., André, J. C., & Villermaux, J. (1988). Investigation of concentration fluctuations in a continuous stirred tank by space-resolved fluorescence spectroscopy. *Proceedings of the Sixth European conference on mixing*, Pavia, 24–26 May (pp. 129–136). Cranfield: AIDIC/BHRA.
- Gaskey, S., Vacus, P., David, R., & Villermaux, J. (1990). A method for the study of turbulent mixing using fluorescence spectroscopy. *Experiments in Fluids*, 9, 137–147.
- Greenhalgh, R. E., Johnson, R. L., & Howard, D. N. (1959). Mixing in continuous reactors. *Chemical Engineering Programme*, 55, 44–48.
- Houcine, I., Vivier, H., Plasari, E., David, R., & Villermaux, J. (1994). Comparison of mixing action of several stirrers by laser sheet visualization and image processing. *Proceedings of the Eighth European conference on mixing*, Cambridge (IChemE Symposium Series Number 136) (pp. 97–104).
- Houcine, I., Vivier, H., Plasari, E., David, R., & Villermaux, J. (1996). Planar laser induced fluorescence technique for measurements of concentration fields in continuous stirred tank reactors. *Experiments in Fluids*, 22, 95–102.
- Kemoun, A., Lusseyran, F., Skali-Lami, S., Mahouast, M., Mallet, J., Lartiges, B. S., Lemelle, L., & Bottero, J. Y. (1997). Hydrodynamic field dependence of colloidal coagulation in agitated reactors. In J. Bertrand & J. Villermaux (Eds.), *Récents Progrès en Génie des Procédés*, Vol. 11(52) (pp. 33–40). Paris: Lavoisier.

- Konishi, Y., Kogasaki, K., & Asai, S. (1997). Bioleaching of pyrite by *Acidianus brierleyi* in a continuous-flow stirred-tank reactor. *Chemical Engineering Science*, 52(24), 4525–4532.
- Magelli, F., Nocentini, M., Orlandini, F., Fajner, D., & Pinelli, D. (1997). Solids separation at the exit of a continuous-flow slurry reactor stirred with multiple axial impellers. *Transactions of the Institution of Chemical Engineers, Part A, Chemical Engineering Research and Design*, 75(1), 284–287.
- Mahouast, M. (1991). Concentration fluctuations in a stirred reactor. *Experiments in Fluids*, 11, 153–160.
- Mahouast, M., David, R., & Cognet, G. (1987). Characterization of hydrodynamic and concentration fields in a continuous fed standard stirred tank, *Entropie* (133), 7–17.
- Mahouast, M., Nardin, P., El Rhassouli, A., & Rondot, D. (1991). Concentration measurements in a stirred tank using fluorescence spectroscopy and image processing. *Proceedings of the Seventh European conference on mixing*, Brugge, 18–20 September (pp. 187–192). Antwerpen: EFCE-KVIV.
- Mavros, P. (2001). Flow visualisation in stirred vessels. Review of experimental techniques. *Transactions of the Institution of Chemical Engineers, Part A, Chemical Engineering Research and Design A*, 79(2), 113–127.
- Mavros, P., Barrué, H., Xuereb, C., Fořt, I., & Bertrand, J. (2000). Effect of axial-flow impeller and feed tube location on flow patterns in continuous-flow stirred tank reactors. *Paper presented at the Fourteenth international congress chemical and process engineering*, CHISA, Prague, 27–31 August, 2000.
- Mavros, P., & Bertrand, J. (2002). Flow visualisation in stirred vessels. Effect of impeller type on the flow patterns induced. *Transactions of the Institution of Chemical Engineers, Part A, Chemical Engineering Research and Design*, submitted for publication.
- Mavros, P., Naude, I., Xuereb, C., & Bertrand, J. (1997). Laser Doppler velocimetry in agitated vessels. Effect of continuous liquid stream on flow patterns. *Transactions of the Institution of Chemical Engineers, Part A, Chemical Engineering Research and Design*, 75, 763–776.
- Mavros, P., Xuereb, C., & Bertrand, J. (1996). Determination of 3-D flow fields in agitated vessels by laser-Doppler velocimetry—Effect of impeller type and liquid viscosity on liquid flow patterns. *Transactions of the Institution of Chemical Engineers, Part A, Chemical Engineering Research and Design*, 74, 658–668.
- Mezaki, R., Mochizuki, M., & Ogawa, K. (2000). *Engineering data on mixing*. Amsterdam: Elsevier.
- Nienow, A. W. (1997). On impeller circulation and mixing effectiveness in the turbulent-flow regime. *Chemical Engineering Science*, 52(15), 2557–2565.
- Patterson, G. K. (1975). Simulating turbulent-field mixers and reactors or taking the art out of the design. In R. S. Brodkey (Ed.), *Turbulence in mixing operations* (pp. 223–275). New York: Academic Press.
- Roustan, M., & Pharamond, J.C. (1988). Agitation et mélange, *Techniques de l'Ingénieur*, A.10, A5900.
- Ruszkowski, S. (1994). A rational method for measuring blending performance, and comparison of different impeller types. In *Proceedings of the Eighth European conference on mixing*, Cambridge, 21–23 September (pp. 283–291). Rugby: IChemE.
- Sano, Y., & Usui, H. (1987). Effects of paddle dimensions and baffle conditions on the interrelations among discharge flow rate, mixing power and mixing time in mixing vessels. *Journal of Chemical Engineering Japan*, 20, 399–404.
- Tatterson, G. B. (1991). *Fluid mixing and gas dispersion in agitated tanks* (p. 235). New York: McGraw-Hill.
- Zannoud, N., Guiraud, P., Costes, J., & Bertrand, J. (1991). Local laser measurements of velocities and concentrations in two continuous systems: A tubular jet-stirred reactor and a stirred vessel. *Proceedings of the Seventh European conference on mixing*, Brugge, 18–20 September (pp. 173–180). Antwerpen: EFCE-KVIV.